



Scan to know paper details and
author's profile

In Silico Identification of Natural Inhibitors Targeting *Helicobacter Pylori* Carboxyspermidine Dehydrogenase: A Computational Study

Alex J Mbise, P.V.Kanaka Rao, F.M.Stanley & M. S Gurisha

University of Dodoma

ABSTRACT

Gastritis, peptic ulcers, and gastric cancer are the most common disorders and the leading cause of death worldwide. *Helicobacter pylori* is a bacterium that has been related to stomach inflammation, Peptic Ulcer, as well as gastric cancer. The current study sought to identify natural inhibitors of the Crystal Structure of Carboxyspermidine Dehydrogenase in a complex with Nicotinamide adenine dinucleotide phosphate (PDB ID: 8H52) with good resolution of 3.10 \AA° and R-value free of 0.047. Bioactive compounds appear to be a potential treatment strategy for inhibiting *H. Pylori*. 1102 Bioactive compounds from blueberry, gooseberry, plum, cantaloupe, celery, lyngniangbru, tea plant, spinach, ginger, turmeric, radish, fenugreek seeds, carrot, and indigo were selected. Before molecular docking, initial selection of the BACs was based on the physiochemical, lipophilicity, water solubility, pharmacokinetics, druglikeness and pharmaceutical chemistry performed by SwissADME. Binding energy calculations and interaction analysis were applied to identify safe and efficient results. 17 Bioactive compounds were found with binding affinities between -7.8 Kcal/mol and -9.9 Kcal/mol. Among 17; curcumin pyrazole, scoparol, tryptanthrin and 4'-O-methylcatechin were found to bind strong in the protein pocket with docking scores of -9.9 Kcal/mol, -9.6 Kcal/mol, -9.5 Kcal/mol, and -9.5 Kcal/mol respectively compared to the control drug Omeprazole (-8.8 Kcal/mol).

Keywords: BACs, *H. pylori*, binding affinities, molecular docking, and MD simulations, traditional medicinal herbs, garboxyspermidine dehydrogenase, peptic ulcers, gastric disorders, therapeutic agents.

Classification: DDC Code: 615.323

Language: English



Great Britain
Journals Press

LJP Copyright ID: 925684
Print ISSN: 2631-8490
Online ISSN: 2631-8504

London Journal of Research in Science: Natural and Formal

Volume 24 | Issue 7 | Compilation 1.0



In Silico Identification of Natural Inhibitors Targeting *Helicobacter Pylori* Carboxyspermidine Dehydrogenase: A Computational Study

Alex J Mbise^a, P.V.Kanaka Rao^a, F.M.Stanley^b & M. S. Gurisha^c

ABSTRACT

*Gastritis, peptic ulcers, and gastric cancer are the most common disorders and the leading cause of death worldwide. *Helicobacter pylori* is a bacterium that has been related to stomach inflammation, Peptic Ulcer, as well as gastric cancer. The current study sought to identify natural inhibitors of the Crystal Structure of Carboxyspermidine Dehydrogenase in a complex with Nicotinamide adenine dinucleotide phosphate (PDB ID: 8H52) with good resolution of 3.10A° and R-value free of 0.047. Bioactive compounds appear to be a potential treatment strategy for inhibiting *H. Pylori*. 1102 Bioactive compounds from blueberry, gooseberry, plum, cantaloupe, celery, lyngniangbru, tea plant, spinach, ginger, turmeric, radish, fenugreek seeds, carrot, and indigo were selected. Before molecular docking, initial selection of the BACs was based on the physiochemical, lipophilicity, water solubility, pharmacokinetics, druglikeness and pharmaceutical chemistry performed by SwissADME. Binding energy calculations and interaction analysis were applied to identify safe and efficient results. 17 Bioactive compounds were found with binding affinities between -7.8 Kcal/mol and -9.9 Kcal/mol. Among 17; curcumin pyrazole, scoparol, tryptanthrin and 4'-O-methylcatechin were found to bind strong in the protein pocket with docking scores of -9.9 Kcal/mol, -9.6 Kcal/mol, -9.5 Kcal/mol, and -9.5 Kcal/mol respectively compared to the control drug Omeprazole (-8.8 Kcal/mol). Molecular dynamic simulation revealed that 4'-O-methylcatechin is stable inside the binding pocket 8H52 and stood out as good candidate in terms of RMSD, RMSF, Hydrogen bonding formation, and radius of gyration, and therefore suggested this bioactive compound could be used as a potential therapeutic agent to cure gastritis and peptic ulcers.*

Keywords: BACs, *H. pylori*, binding affinities, molecular docking, and MD simulations, traditional medicinal herbs, garboxyspermidine dehydrogenase, peptic ulcers, gastric disorders, therapeutic agents.

Author ^a & ^b: Department of Physics, College of Natural and Mathematical Sciences, University of Dodoma, Tanzania, P. O. Box 338 Dodoma, Tanzania.

^c: Tanzania Atomic Energy Commission, P.O. Box 743 Arusha, Tanzania.

I. INTRODUCTION

The prime reservoir of bacteria in humans is in the digestive tract and *Helicobacter pylori* (*H. pylori*) is one of the threats leading to ulcers. *H. pylori* has the capacity to endure in the hostile environment of the stomach (Fagoonee & Pellicano, 2019). Moreover, *H. pylori* has become one of the most prevalent infections in humans and a major causative factor in a number of stomach conditions, such as gastritis, peptic ulcers, and gastric carcinoma (Haley & Gaddy, 2015). People diagnosed with *H. pylori* are expected to have a more than twice higher risk of developing gastric cancer relative to non-infected individuals (Queiroz et al., 2012).

1.1 Level of *H. pylori*

Proportionally, the major affected population with *H. pylori* has been falling in the Western world with high levels of industrialization around the turn of the twenty-first century, whereas it has stagnated at high levels in developing and recently industrialized nations. *H. pylori* occurs more frequently in Asia, Latin America, and Africa than in North America and Oceania, where it has been discovered in only 24% of the population (Sjomina et al., 2018) (FitzGerald & Smith, 2021) (Elbehiry et al., 2023). 50.8% of people with *H. pylori* infection reside in developing countries compared to 34.7% in industrialized countries (Elbehiry et al., 2023). The future global occurrence of disorders related to *H. pylori*, such as peptic ulcer and gastric cancer, will be significantly impacted by the increasing industrialization (Hooi et al., 2017).

1.2 The virulence of *H. pylori*

This bacteria (*H. pylori*) is a gram-negative bacterium with a helical structure that colonizes the human gastrointestinal tract, especially leading to infection of the stomach epithelium (Charitos et al., 2021). Four essential steps are necessary for *H. pylori* bacteria to achieve effective colonization, persistent infection, and disease pathogenesis once they have entered the stomach of the host: (a) survival in the stomach's acid; (b) motility toward epithelial cells via flagella; (c) adhesion/receptor contact for attachment to host cells; and (d) release of toxins that cause tissue damage (Kao et al., 2016). Infection normally causes silent stomach inflammation, but chronic exposure to more pathogenic strains causes serious pathological changes such as gastric and duodenal ulcers, as well as tumor progression that ends in gastric malignancies and carcinoma (Peek & Blaser, 2002). Gastric and duodenal ulcer wounds are at least 5 mm broad but can be much larger and deeper ulcers involving the capillaries of the muscularis propria and even the serosa layer can induce bleeding and perforation, although ulcers in the pyloric canal can produce pyloric smooth muscle spasm, resulting in pyloric obstruction (Gurusamy & Pallari, 2016).

An enzyme known as urease is produced by *H. pylori*. Due to its weakening effect on the gastric lining, this enzyme neutralizes and acidity of stomach acids and help *H. pylori* survival before the mucous layer. A thick coat of mucous coating the stomach wall shields it against its own gastric acid (Penta et al., 2005). Mucins, which are high molar mass and extensively glycosylated glycoproteins, form the mucous membrane and protect stomach epithelial cells. The primary mucins produced in the stomach are MUC 1 (membrane-bound) and MUC5AC and MUC6 (secreted), MUC5AC, constituting the majority of the adherent unstirred mucus layer, is released by surface foveolar cells. In contrast, MUC6 is released by neck and gland cells, and both are highly expressed in normal stomach lining (Boltin & Niv, 2013). *H. pylori* enzymes, protease and lipase, break down gastric mucus and disrupt the phospholipid-rich layer on the surface of apical epithelial cells, permitting gastric epithelium cells damage from the backward flow of gastric acid (Smoot, 1997). The mucosal layer's primary elements are associated with *H. pylori* and aid in the bacterium's adhesion to the gastric epithelium (Van den Brink et al., 2000). The role of this pathogen in stomach disorders remains uncertain and controversial. *H. pylori* induces passive inflammation in the gastric epithelium and disrupts signal transduction pathways, which facilitates pathogenesis. Additionally, it acquires antimicrobial resistance through genetic changes and biofilm formation (Baj et al., 2020) (Elbehiry et al., 2023).

8H52 is the crystal structure of *Helicobacter pylori* carboxyspermidine dehydrogenase (CASDH) in combination with Nicotinamide adenine dinucleotide Phosphate (NADP). This protein contains spermidine, a positive polyamine that is important in a variety of biological activities. CASDH aids *H. pylori*'s survival and virulence by enabling the metabolism of polyamines, which are essential for the bacterium's growth, stress response, and ability to colonize the acidic stomach environment. (Ko et al., 2022). To biosynthesize spermidine, *H. pylori* uses the enzymes CASDH and carboxyspermidine

decarboxylase (CASDC), the presence of spermidine is necessary for bacterial growth (Zhang & Au, 2017).

1.3 Herbs bioactive compounds (BACs) and drug designing

The usage of phytochemicals, often known as nutritional supplements, is growing faster all over the world for treating a variety of health issues (Organization, 2004). Numerous substances originating from natural sources have shown pharmacological properties against *H. pylori*, which makes them extremely promising candidates for future medication. These medicines derived from plants are largely used and are a better option due to safety in use, availability, and have few side effects compared to the synthetic alternatives (Iwu et al., 1999).

Drug designing is an important area of research where computational biophysics, biochemistry, and data science have recently gained popularity and the use of computational methods can assist researched results from sizable databases and synthesized new tiny molecules (Preman et al., 2022). Computer-aided drug design (CADD) has gained general recognition among scientists as part of a comprehensive drug-designing strategy (Sabe et al., 2021). Therefore, this work focused on uncovering new possible leads from herbs that could be used to inhibit spermidine production in battling *H. pylori* using computational methods, which is a major cause of gastritis, peptic ulcers, and gastric cancer.

II. METHODOLOGY

2.1 Protein Preparation

The crystal structure CASDH from *H. pylori* in combination with NADP (PDB ID: 8H52) was retrieved from Protein Data Bank (<https://www.rcsb.org/>). NADP alters the structure ordering of carboxyspermidine dehydrogenase by optimizing its configuration for efficient catalysis in polyamine metabolism, thereby enhancing the protein's functional activities crucial for cellular processes. (Ko et al., 2022). Protein was prepared in to receptor by the addition of charges, polar hydrogen, and deletion of the heavy atoms, including co-crystallized ligands, water molecules, heteroatoms, Actosite, and co-factors. And the addition of polar Hydrogen took place performed in BIOVIA discovery and UCSF Chimera with charmm force field parameter to perform energy minimization of the receptor.

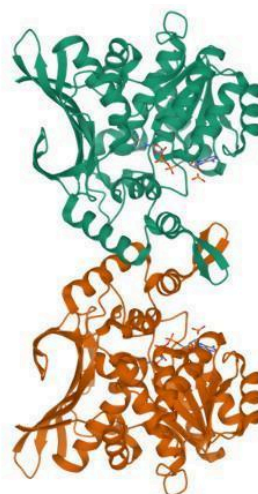


Figure 1: Helicobacter pylori carboxyspermidine dehydrogenase crystal structure in combination with NADP (PDB ID: 8H52)

2.2 Ligand Preparation and Virtual screening

The Zinc Data Base was used to obtain all-natural chemical structures (ligands) in SDF format. Before molecular docking, ligands were filtered by druglikeness for the preliminary assessment of physiochemical, pharmacokinetic, and ADMET properties performed in SwissADME. The ligands preparation and virtual screening were done in PyRx 0.9x and UCSF chimera software with an Autodock vina to find the BACs fit to the target and acquire a variety of binding conformations and binding affinities (BA) by approximates the Gibbs free energy change upon binding. Table 1 represents the alternative medicines uses or other biological activities.

Table 1: Complementary medicine uses, herbal sources and selected BACs

Major BACs chosen for anti-peptic ulcers	Source of BACs	Complementary medicine uses
Hydroxybenzoic acid, Hydroxycinnamic acid, Cyanidin, Delphinidin, Malvidin, Peonidin, Petunidin, Pelargonidin and Procyanidin B1, Procyanidin B2, Procyanidin B3, Procyanidin A1, Procyanidin A2 and Proanthocyanidins (Tannins)	<i>Ribes uva-crispa</i> and <i>Vaccinium sect. Cyanococcus</i>	Enabling digestion, lower fever, detoxify blood, lower cough, significant for eyes, enhance hair growth (Annapurna, 2012)
Isoflavonoids, Dihydroflavanols, Dihydrochalcone, Cinamic acid, Feruloylquinic acid, Comaroylquinic acid, Shikimic acid, Ellagic acid, Propionic acid, Abscisic acid, β -carotene and α -carotene.	<i>Prunus Domestica</i>	Anti-cancer, Anti-bacteria, Anti-fungal (Hussain et al., 2021)
β -carotene, α -carotene, Hydroxybenzoic acid, Hydroxycinnamic acid, dehydroascorbic acid (DAA), Chlorophyll, lycopene, lutein, Ellagic acid, Gallic acid, Kaempferol, xanthophyll and flavonoids	<i>Cucumis melo var. cantalupensis</i>	Anti-oxidant, Anti-microbial, maintain radical stability, anti-carcinogenic (Vella et al., 2019)
Cyanidin, Chlorogenic acid, apigenin, apiai, Rutin, niacin, riboflavin, pantothenic acid, choline, phylloquinone, dehydroascorbic acid (DAA), Vitamin E succinate, oleic acid, β -linoleic acid, α -linoleic acid, (3,7-dihydroxyflavonoid), Cirtusin A, Abietin, Peucedanin, Citropten, Ostheno, Xanthophyll, diadinoxanthin, violaxanthin, artemisin, ganoderic acid V, ganoderic acid R, α -ionone, diosmetin, tomatine, corticocin, and saffloomin A	<i>Apium graveolens</i>	Anti-oxidants, Anti-microbial, hypolipidemic, hypoglycemic, and anti-platelet aggre(Sowbhagya, 2014)
Epicatechin, Quercetin, Kaempferol, Galic acid, Ellagic acid, Caffeic acid (Hydroxycinnamic acid)	<i>Potentilla Fulgens</i>	Antimicrobial, anticancer, antioxidant, anti-inflammatory, and antiulcerogenic, as well as anti-hyperglycemic, anti-hyperlipidemic(Nath & Joshi, 2013)
Catechin, Theaflavin, flavonol glycosides, L-theanine, Caffeine, theobromine.	<i>Camellia sinensis</i>	Therapy of cardiovascular conditions, cancer, digestive issues, obesity, and diabetes. Also show strong anti-oxidants, and

		anti-inflammatory attributes (Samanta, 2022)
Hydroxybenzoic acid, Hydroxycinnamic acid, Flavonoids and Carotenoids	<i>Spinacia oleracea</i>	Anti-tumor, Antioxidant, bile acid binding, and Anti -inflammatory actions (Singh et al., 2018)
Gingerols, Shogaols, Paradols, Quercetin, Zingerone, Gingerenone-A, 6-dehydrogingerdione, β -bisabolene, α -circumene, Zingiberene, α -farnesene, β -sesquiphellandrene.	<i>Zingiber officinale</i>	Gastrointestinal protection, cholesterol lowering, anti-obesity, cardioprotective, anti-diabetic, anti-inflammatory, and anti-cancer activities and digestive stimulant (Srinivasan, 2017)
Demethoxycurcumin, bisdemethoxycurcumin, Ar-turmerone, α -phellandrene, Terpineole, α -zingiberene, β -sesquiphellandrene, Ar-turmerol, farnesol, β -bisabolol, Germacrone, Caffeic acid, Catechin, Chlorogenic, Cinnamic acid, Myricetin, Rutin, Quercetin, Sinapic acid, curcumin pyrazole, and Vanilic acid	<i>Curcuma</i>	Antioxidant qualities, anti-inflammatory properties, anti-cancer properties, neuroprotective properties, antibacterial and antiviral effects, asthma and diabetes prevention properties (Sahoo et al., 2021)
Ascorbic acid, α -tocopherol, Glucoraphanin, 4-hydroxyglucobrassicin, Neoglucobrassicin, Sulforaphene, Sulforaphane, Indole-3-carbinol	<i>Raphanus sativus</i>	Prevention of cancer by apoptosis, Inhibit growth of H.Pylori due to antioxidants presence, therefore lower the risk of Gastric cancer (Lim et al., 2015)
vitexin-7-O-glucoside, vicenin-2, vicenin-2, orientin, luteolin, naringenin, quercetin, diosgenin, yamogenin, yuccagenin, tigogenin, and smilagenin	<i>Trigonella foenum-graecum</i>	Gastroprotective, anti-hypercholesterolemic Preventing liver damage, Stabilize blood glucose level, cytotoxic (Olaiya & Soetan, 2014)
β -carotene, Tocopherol, Xanthophyll, Lutein, Chlorogenic acid, Falcarinol, Falcarindiol, Falcarindiol-3-acetate, Glutamic acid, Caffeic acid, Thiamin, Riboflavin, Niacin.	<i>Daucus carota</i>	Antitumor, cytotoxic, anti-inflammatory, cardiovascular diseases (Ahmad et al., 2019)
Alkaloid (Tryptanthrin), Flavanoids, terpinoids, Indigotine, Indurubens and ratenoids.	<i>Indigofera tinctoria</i>	Anti-viral, Anti-bacterial, Anti-inflammatory, Gastroprotective also prevent liver damage (Motamarri et al., 2012)

2.3 Molecular docking

The AutoDock Vina tool was used to dock the selected BACs with the crystal structure of Carboxyspermidine dehydrogenase from *Helicobacter pylori* in combination with NADP, with Vina search center (X: -16.2076, Y: -29.6123 and Z: -24.0957) and Dimension (Angstrom) (X: 71.9734 Y: 47.2377 Z: 74.8061) using PyRx, and the best responses were subjected to site specific docking using UCSF chimera with coordinates center (X: -37, Y: 4, and Z: -18) and coordinate size (X: 10, Y: 22, and Z: 15). Center coordinates target binding site by center the box on the known or predicted binding site of the target protein, while dimensions ensuring entire binding pocket is covered, including possible

sub sites which allow ligands to explore all potential binding conformation with the binding site (Zhao et al., 2020). Hydrogen bonds interaction, hydrophobic interaction, solvation effects and binding affinities scores estimated by autodock vina provide the optimal conformation with lowest docking potential and best poses. The potential scores with best poses were picked for visualization and interaction analysis using Maestro (reddy Peasari et al., 2018) and UCSF Chimera (Pettersen et al., 2004).

2.4 Physicochemical, Pharmacokinetics, and Drug Likeness Aspects of BACs

Typical computational pharmacokinetics parameters and drug-likeness were developed for the assessment of physicochemical, pharmacological, and drug-like features during the drug development process. Ghose, Veber, Egan, and Muegge rules are characteristics of drug likeness that define Lipinski (Lipinski, 2004). Any bioactive compound potential for treatment has to obey Lipinski's rule of five and the data from the ADMET investigations were filtered and confirmed for Lipinski's rule of five that are stated as follows: hydrogen-bonding donors < 5 (the overall amount of nitrogen-hydrogen and oxygen-hydrogen bonds), hydrogen bond acceptors < 10 (all nitrogen or oxygen atoms), a molecular weight < 500 daltons, and a coefficient of octanol-water partitioning $\log P < 5$ (Lipinski, 2004). The first two rules for Hydrogen bond donor and acceptor imply adequate intestinal availability, and the latter two rules imply excellent oral absorption thus this decides whether a molecule is drug-like or not (Schneider, 2013) (Lipinski, 2004). All BACs were ADME/T screened using the internet web SwissADME to determine the drug-likeness agents (Bakchi et al., 2022).

2.5 MD modeling of protein-ligand interactions

Molecular Dynamics Simulation was conducted to understand in deep how 8H52 interacts with potential phytochemicals when it binds to a target protein, molecular dynamics (MD) simulation aids in the visualization of protein flexibility (Hansson et al., 2002). Analyzing the underlying motions of protein-ligand complexes can reveal several new unexplored bioactivities and intricate dynamic processes (Anwer et al., 2015). GROMACS was utilized to investigate the stability of the complexes, energy minimization, and equilibration (Gapsys et al., 2022). The GROMACS was also utilized in the simulation of Receptor-ZINC519621, Receptor-ZINC33299, Receptor-ZINC14642912, and Receptor-ZINC19816066 at 300K, with CHARMM27 force fields then hybrid ligand structure and force field properties of chosen ligands were determined using Swiss Param

In a "cubicbox" with a basic diameter of 1 nm with all the default settings, Receptor-ZINC519621, Receptor-ZINC33299, Receptor-ZINC14642912, and Receptor-ZINC19816066 were wet. The heat of all systems was raised from 0 to 300 K during the length of the equilibration time (1000 ps), while preserving a steady volume and periodic boundary conditions, and the system was then reduced using 1000 "sharpest decline" steps. The resulting trajectories were utilized to examine the system stability as well as to evaluate each complex's behavior. Root mean square deviation (RMSD), root mean square fluctuation (RMSF), radius of gyration (Rg), Hydrogen bonding (H-bond), and Total energy calculations were used to examine the variations of the macromolecule and macromolecule-ligand complex system (Salaria et al., 2022).

NVT ensemble and NPT ensemble were the two phases of the equilibration process. While all other atoms were allowed to move freely in both NVT and NPT, the C backbone atoms of the original structures were constrained. The MD was then run at 300 K with a 10 ns time frame. The obtained trajectories were examined using GROMACS analysis modules. UCF Chimera and Maestro were used to produce MD movies and interaction diagrams respectively.

III. RESULTS AND DISCUSSION

This study tested 1102 BACs derived from traditional herbs with the goal of targeting spermidine, which is biosynthesized by carboxyspermidine dehydrogenase (CASDH) in *H. pylori*. Initially, 323 BACs found to have druglikeness after filtering physicochemical, lipophilicity, water solubility, pharmacokinetics and medicinal chemistry. Four BACs were found to have significance scores from molecular docking for the inhibition of 8H52 protein. These were curcumin pyrazole (ZINC19816066), scoparol (ZINC519621), tryptanthrin (ZINC33299) and 4'-O-methylcatechin (ZINC14642912). Curcumin pyrazole was from *curcuma*, scoparol from *trigonella foenum-graecum*, tryptanthrin from *indigofera tinctoria*, and 4'-O-methylcatechin from *camellia sinensis* and *curcuma*. Spermidine is significant for bacteria growth and cell survival. Therefore *H.pylori* binds on the surface and facilitates adherence to the gastric epithelial cells. These bioactive substances were observed to be crucial for the suppression of spermidine to stop the protein's development. The physicochemical, pharmacokinetic, drug-likeness, and ADMET aspects of curcumin pyrazole, scoparol, tryptanthrin, and 4'-O-methylcatechin are presented in Table 2.

Table 2: ADME evaluation of curcumin pyrazole, scoparol, tryptanthrin and catechin

Property	Attribute	Value				Unit
		Curcumin pyrazole ZINC19816066	Scoparol ZINC519621	Tryptanthrin ZINC33299	Catechin ZINC14642912	
Physicochemical	Molecular weight	364 27	300.26 22	248.24 19	290.27 21	g/mol
	Number of heavy atoms	17	16	16	12	
	Number of aromatic heavy atom	6	2	0	1	
	Number of rotatable bonds	5	6	3	6	
	Number of H-bond acceptors	3	3	0	5	
	Number of H-bond donors					
	Molar Refractivity	106.36	80.48	70.77	74.33	
Lipophilicity	$\log P_{o/w}$	3.12	2.18	2.08	0.85	
Water solubility	$\log S$ Solubility Class	-4.73 6.83e-03; 1.88e-05 Moderately soluble	-4.06 2.61e-02; 8.69e-05 Moderately soluble	-2.77 4.22e-01; 1.70e-03 Soluble	-2.14 2.09e+00; 7.19e-03 Soluble	mg/ml; mol/l
Pharmacokinetics	GI absorption	High	High	High	High	
	BBB permeant	No	No	Yes	No	
	P-gp substrate	No	No	No	No	
	CYP1A2	Yes	Yes	No	No	
		No	Yes	No	No	

		CYP2C19 CYP2C9 CYP2D6 CYP3A4 <i>Log K_p</i>	No -5.64	Yes -5.93	Yes -6.36	No -7.82	cm/s
Druglikeness	Lipinski Ghose Veber Egan Muegge Bioavailabilit y score	Yes; o violation Yes Yes Yes Yes 0.55	Yes: o violation Yes Yes Yes Yes 0.55	Yes: o violation Yes Yes Yes Yes 0.55	Yes: o violation Yes Yes Yes Yes 0.55	Yes: o violation Yes Yes Yes Yes 0.55	
Pharmaceutical Chemistry	PAINS Brenk Lead likeness Synthetic accessibility	o alert o alert MW>350 3.14	o Alert o Alert Yes 3.06	o Alert o Alert MW< 250 2.42	o Alert o Alert 2.42	1 Alert 1 Alert Yes 3.50	

These four BACs were found to have the highest binding scores as compared to the synthetic medicine omeprazole, with a binding affinity of -8.8 Kcal/mol. Curcumin pyrazole from curcuma has the highest docking score of -9.9 Kcal/mol, scoparol from trigonella foenum-graecum exhibits favorable interaction with a docking result of -9.6 Kcal/mol, followed by tryptanthrin from indigofera tinctoria and 4'-O-methylcatechin from camellia sinensis and curcuma which has -9.5 Kcal/mol.

Curcuma possesses antioxidant, anti-inflammatory, anti-cancer, neuroprotective, antibacterial, and antiviral properties, as well as asthma and diabetes-preventative characteristics (Sahoo et al., 2021), curcumin pyrazole formed π - π stacking bonding with PHE183. Furthermore, curcumin pyrazole formed three hydrogen bonds (H-bonds) with the receptor's residues. The H-bonds was formed with ASH143, LEU85, and SER34. The ASH143 and SER34 are the hydrogen bond acceptors (HBA), and LEU85 is the hydrogen bond donor (HBD). H-bonds are important for the stability of the complex structure and also for drug absorption and distribution (Coimbra et al., 2021). Atoms exposed to solvent for curcumin pyrazole from the 2D interaction diagram are C19, C20, C21, C2, O1, C1, C7, C9, C11, C13, C14 and C17 as depicted in Figure 2 (a and b).

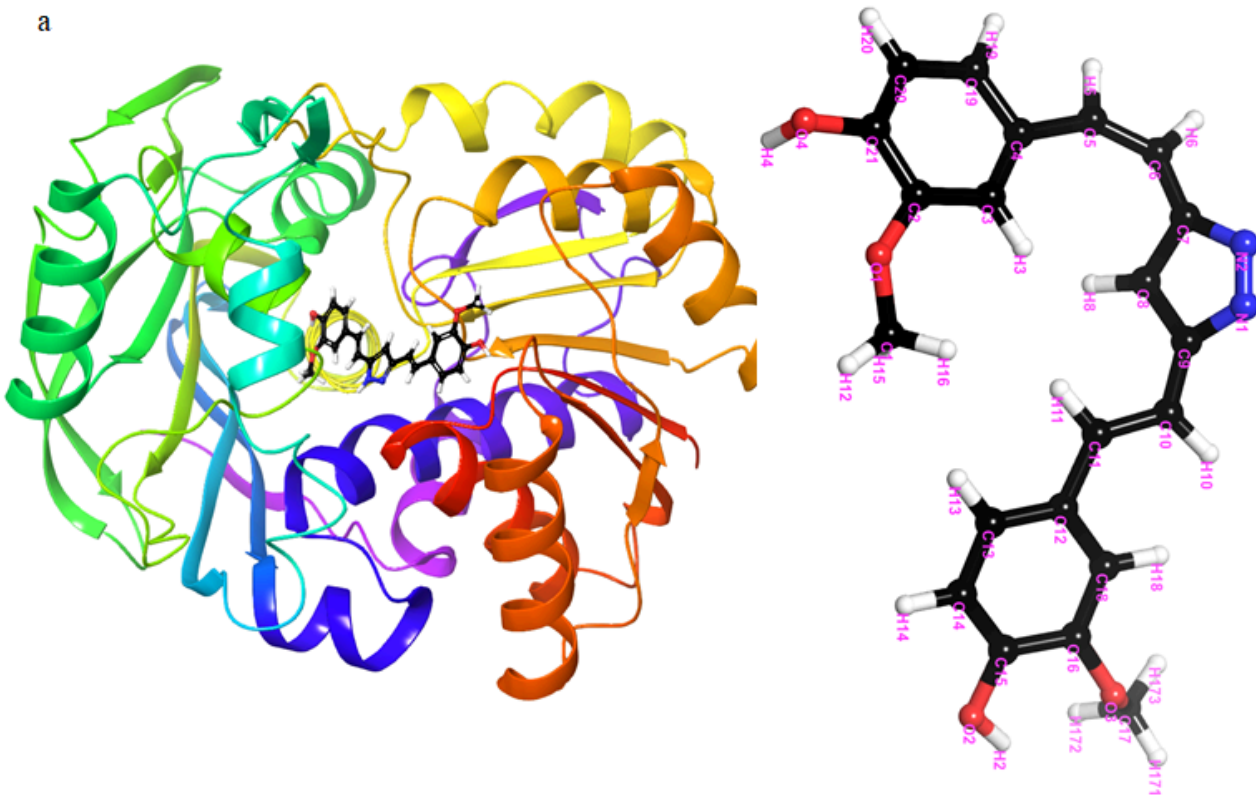


Figure 2 a: 3D visualization of receptor-curcumin pyrazole and curcumin pyrazole structure.

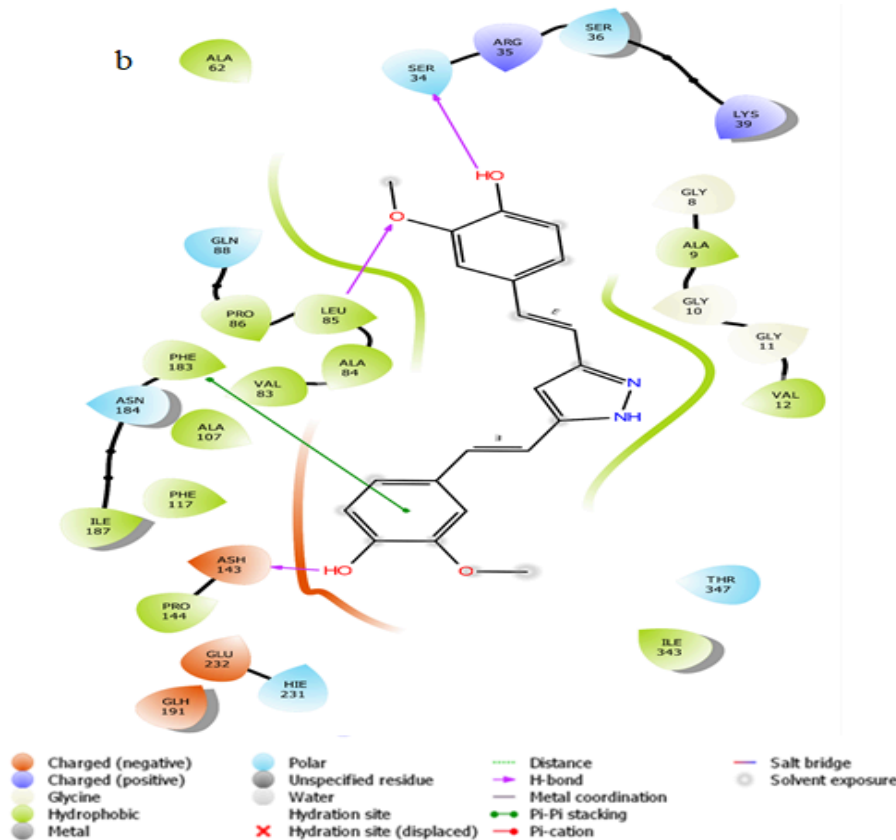


Figure 2 b: 2D interaction diagram of curcumin pyrazole inside binding pocket of 8H52

Scoparol during docking produces two different pose structures which are visualized in 2D interaction. Figure 3b, initially, the 2D interaction diagram of scoparol shows scoparol formed two π - π stacking

with residue PHE183, and four H-bonds with ASH143, GLH191, GLU232, and VAL83. In these configurations ASH143, GLU232, and VAL83 were HBAs while GLH191 was HBD. The final structure in Figure 3c, scopolol formed two π - π stacking with residue PHE183, and three H-bonds with GLH191, GLU232, and VAL83. In this interaction diagram GLU232 and VAL83 are HBAs while GLH191 is the HBD. In the first pose structure, solvent exposure of scopolol atoms inside the receptor is observed in Figure 3b in the ring with C12, C11, C8, and O6. For the second pose structure, in Figure 3b, atoms C12, C11, O5, and O6 are exposed to solvent as depicted in scopolol atoms in Figure 3a.

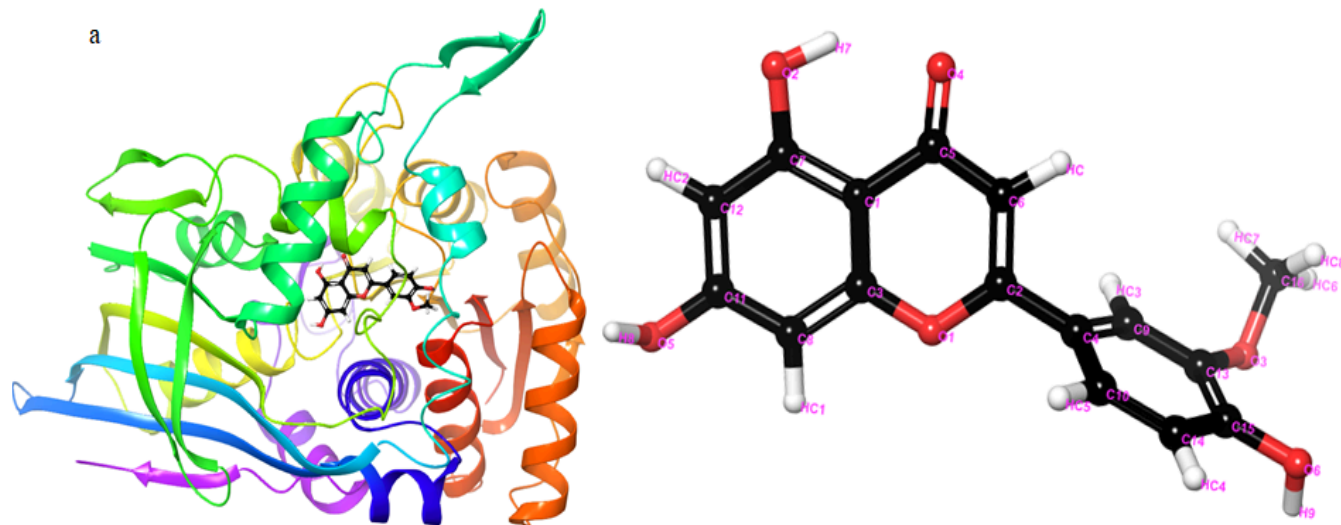


Figure 3a: 3D visualization of receptor-scopolol and scopolol structure.

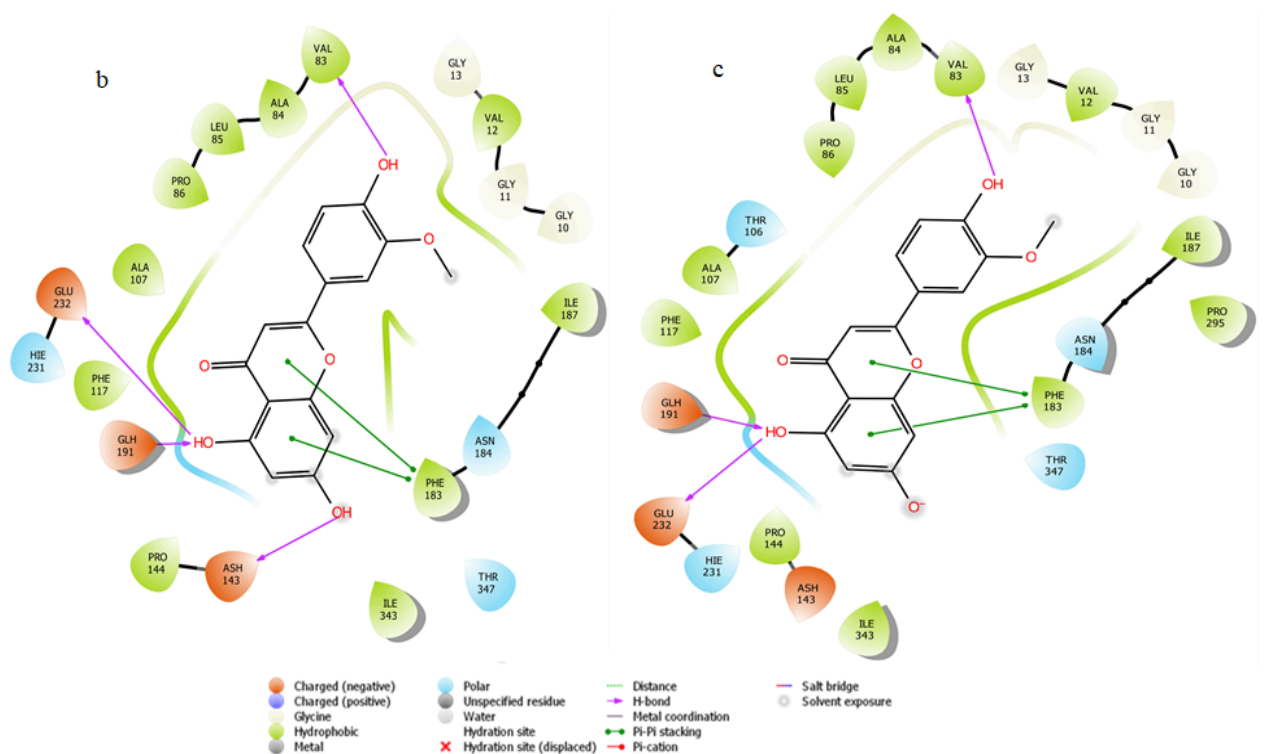


Figure 3 (b and c): 2D interaction diagram of two different poses of scopolol inside the binding pocket of 8H52

It has been found that *indigofera tinctoria* contains antiviral, antibacterial, anti-inflammatory, and gastroprotective properties that also inhibit liver damage (Motamarri et al., 2012). Tryptanthrin formed two π - π stacking bonds with the PHE183. Moreover, there is one hydrogen bond with GLH191, in which GLH191 is the HBD. It is also observed that C11, C12, C13, C15, and C14 are exposed to solvents compared to other atoms as shown in Figure 4 (a and b).

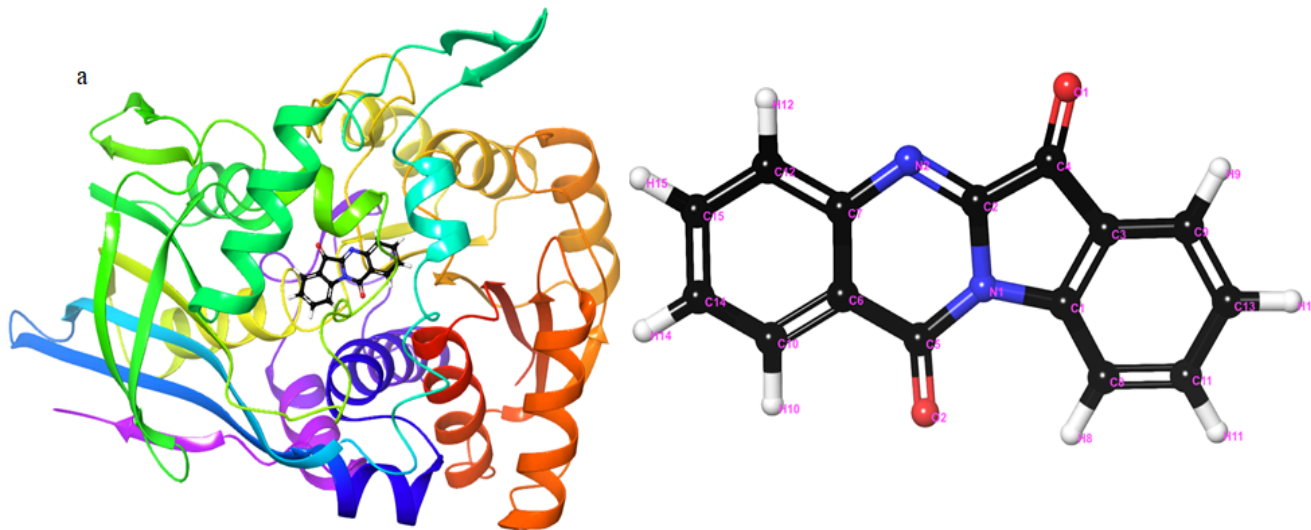


Figure 4a: 3D visualization of receptor-tryptanthrin and tryptanthrin structure

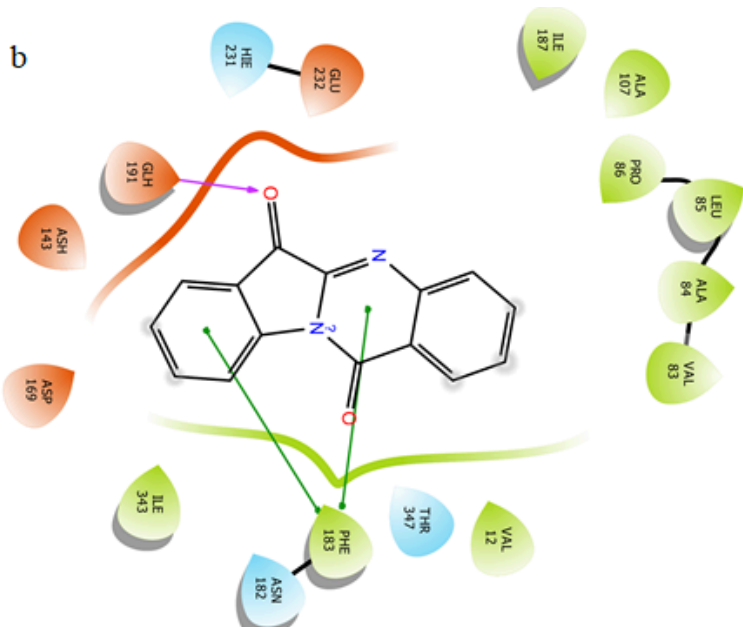


Figure 4b: 2D interaction diagram of tryptanthrin inside the binding pocket of 8H52

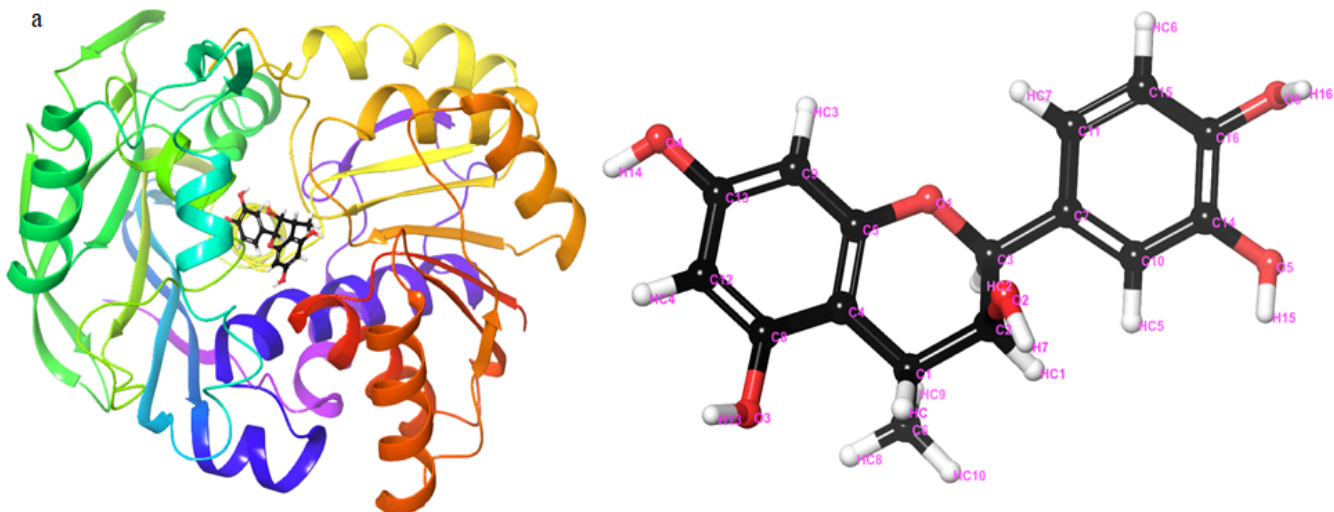


Figure 5 a: 3D visualization of receptor-4'-O-methylcatechin and 4'-O-methylcatechin structure.

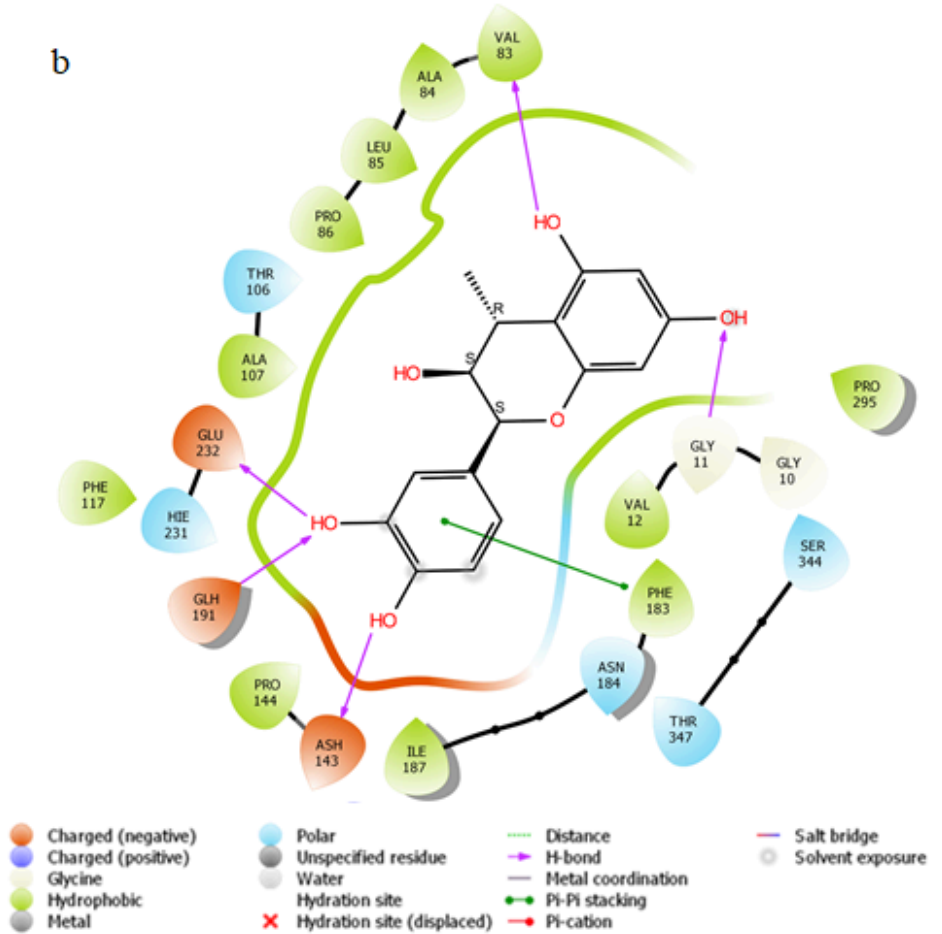


Figure 5 b: 2D interaction diagram of 4'-O-methylcatechin inside binding pocket of 8H52

Antioxidants, anti-inflammatory, gastrointestinal protection, and antitumor activities have also been reported from *Camellia sinensis* and *Curcuma* (Sahoo et al., 2021; Samanta, 2022). 4'-O-methylcatechin formed π - π stacking bonding with PHE183, in this there are five hydrogen bonds formed with the residues. Three are HBAs, ASH143, VAL83, and GLU232; while the GLY11 and GLH191 are HBDs. This contributes to the overall binding affinity of the 4'-O-methylcatechin inside the

protein structure. It is shown also that C15, C16, and C14 are exposed to solvent compare to other 4'-O-methylcatechin atoms as shown in Figure 5 (a and b).

H. Pylori has been becoming resistant to a number of synthetic drugs that are used as a therapy (Qureshi & Graham, 2000). One of the commonly used therapeutic drugs which is widely used for inhibition of *H. Pylori* is Omeprazole. From the docking result of Omeprazole against the target (8H52), the binding affinity was observed to be 8.8Kcal/mol. It was observed that, omeprazole had no bonds formed with the residues. As seen from Figure 6, C12, C14, C13, O1, C4, S1, C2, C3, C6, C8, C11, and C16 are exposed to solvent.

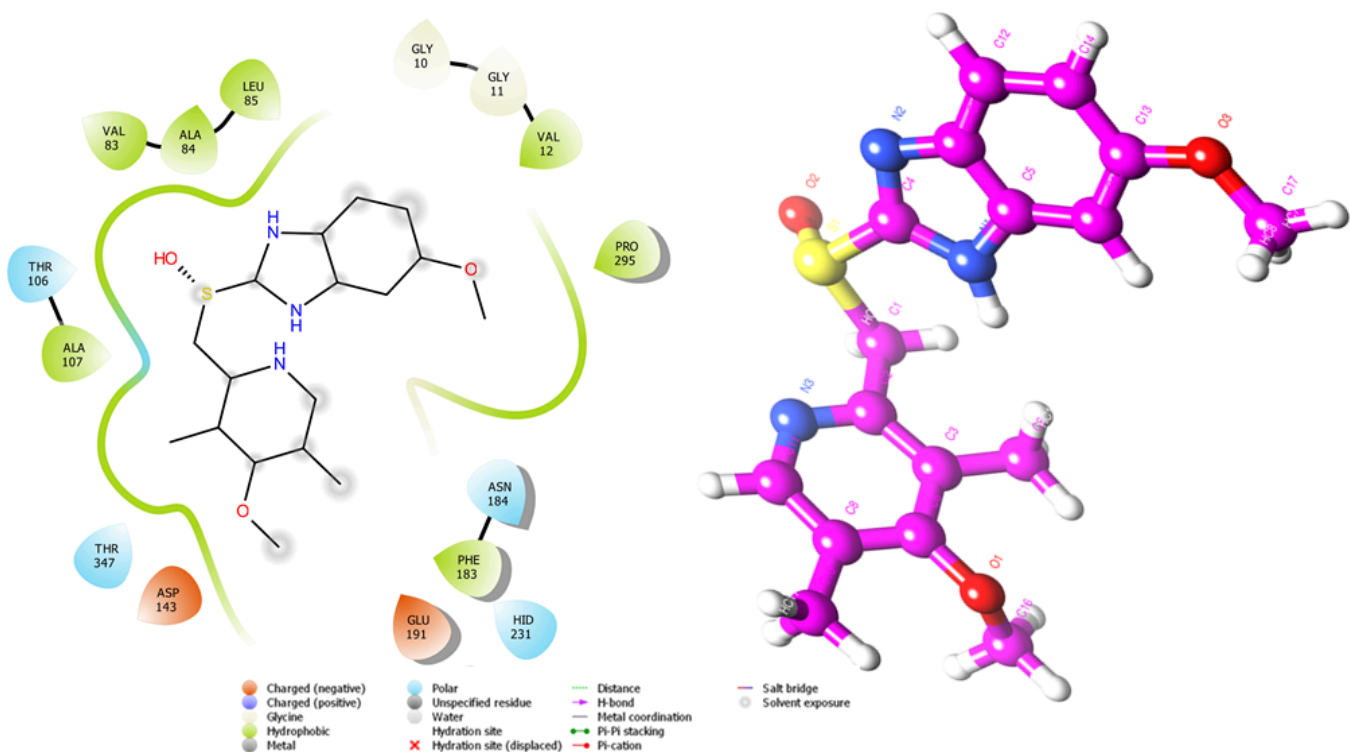


Figure 6: 2D interaction diagram of omeprazole inside binding pocket of 8H52

Inhibiting Spermidine, which is essential for bacterial biofilm development and cell growth, is as important as for bacterial ablation because it prevents bacterial adherence to stomach epithelial cells. Thus, the receptor-ligand interaction is a promising technique for *H. pylori* suppression in the prevention of peptic ulcers and gastric cancer. It has been observed that curcumin pyrazole, scoparol, tryptanthrin, and 4'-O-methylcatechin interact well with 8H52, and the interesting is the formation of H-bonds that maintain the stability of the complexes. RMSD analysis was employed to assess the stability of the protein-ligand complex throughout a defined time period of 10 ns. This was an essential metric in determining structural stability. Findings from molecular dynamic simulation indicated that the mean stabilities of the studied protein-ligand complexes have been found to be 0.42 nm for 8H52-curcumin pyrazole, 0.39nm for 8H52-scoparol, 0.395nm for 8H52-triptanthrin, 0.18nm for 8H52- 4'-O-methylcatechin, while it was 0.56 nm for 8H52-Omeprazole. Analysis from RMSD indicated that the maximum deviation exhibited by OM (omeprazole) and CP (curcuminpyrazole) was 0.63 nm and the minimum deviation was shown by CA (4'-O-methylcatechin) with the value of 0.18 nm. This shows that 4'-O-methylcatechin has good stability compared to the four ligands as depicted in the line and box plot (Figure 7) (Castro-Alvarez et al., 2017). Furthermore, the total energy interaction

profile for the five ligands is less ranged from -480000 KJ/mol to -478300 KJ/mol. This indicating that the system is stable during the simulation (Figure 8) (Peach et al., 2017).

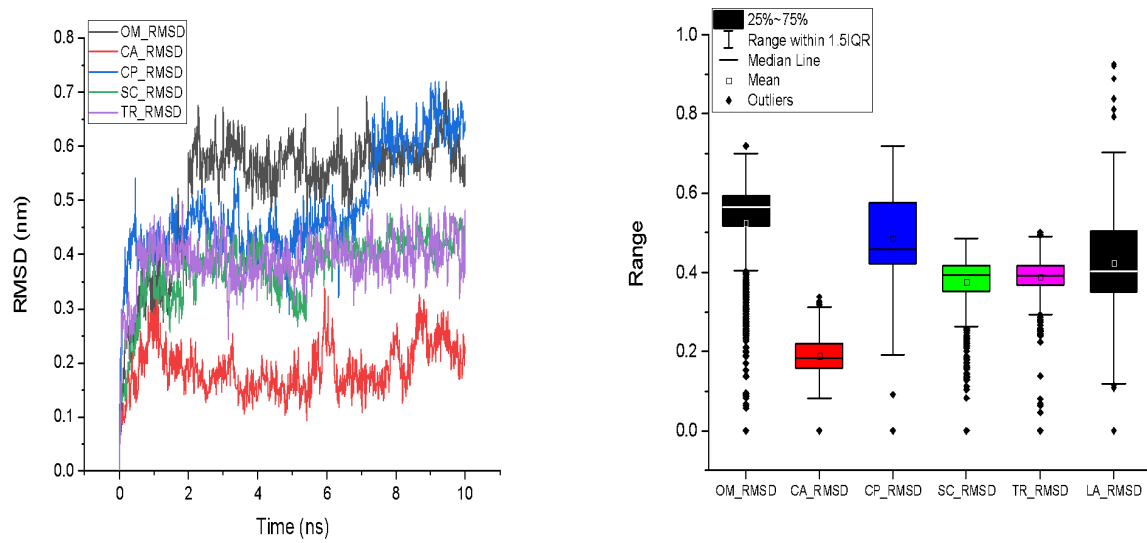


Figure 7: RMSD plot of BACs and control drug in complexation with 8H52

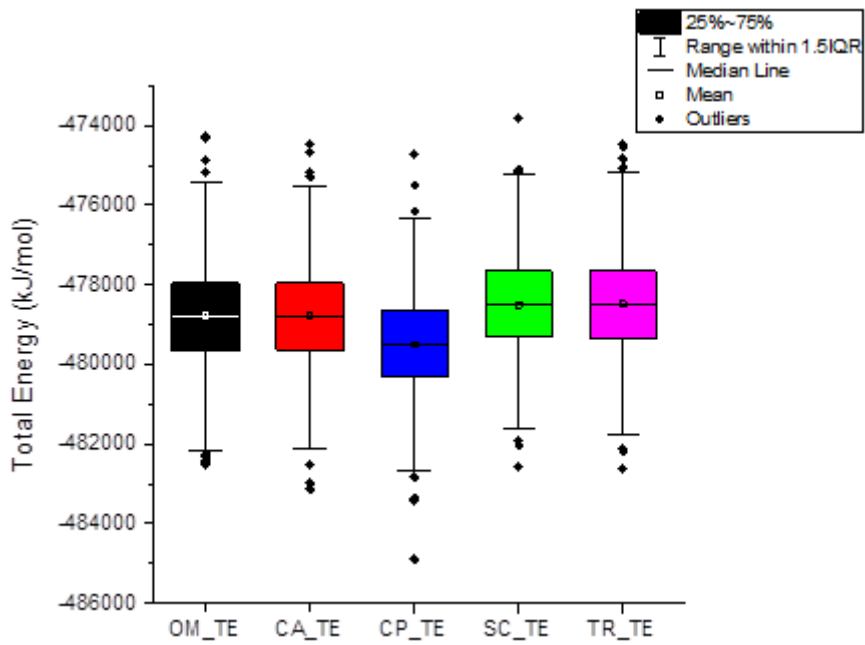
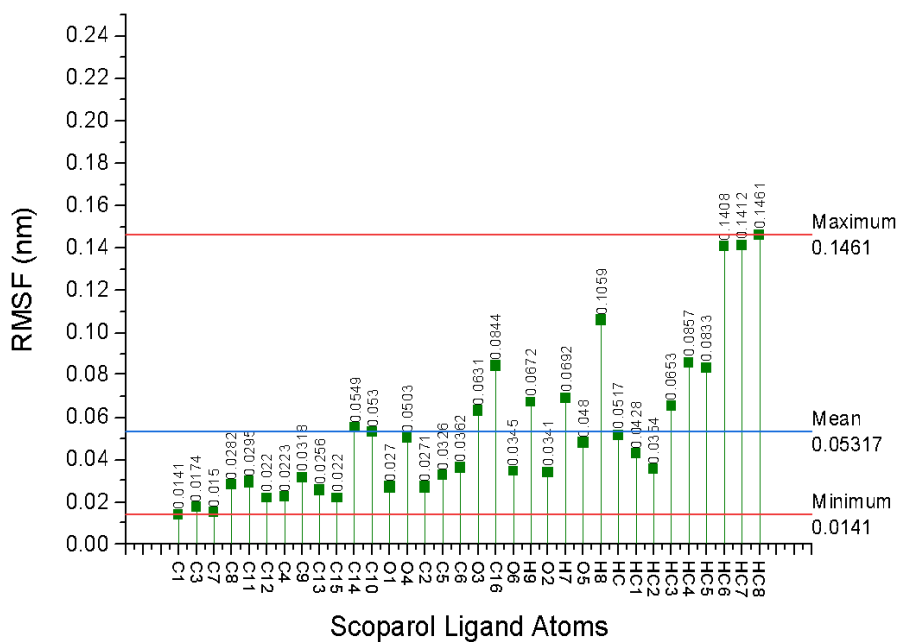
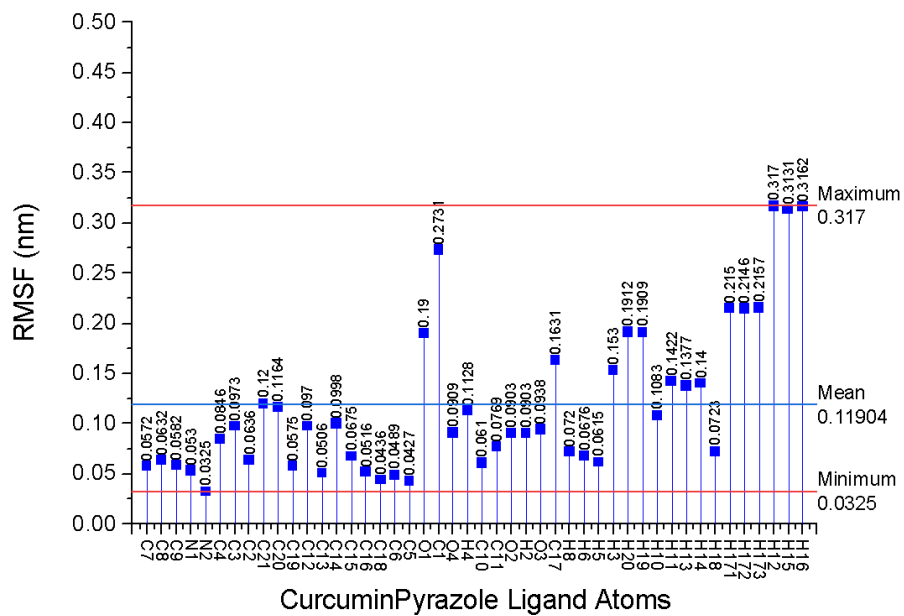
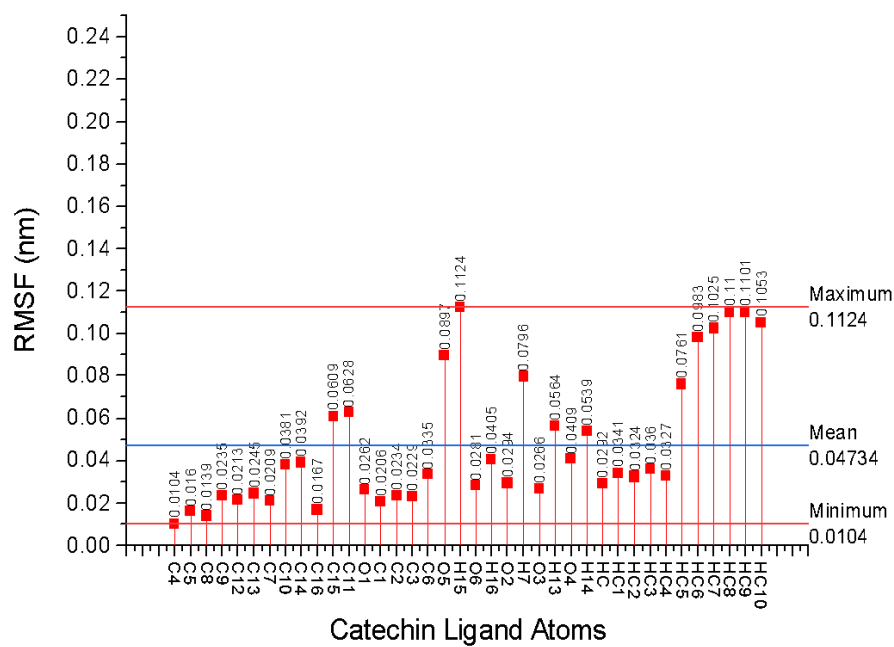
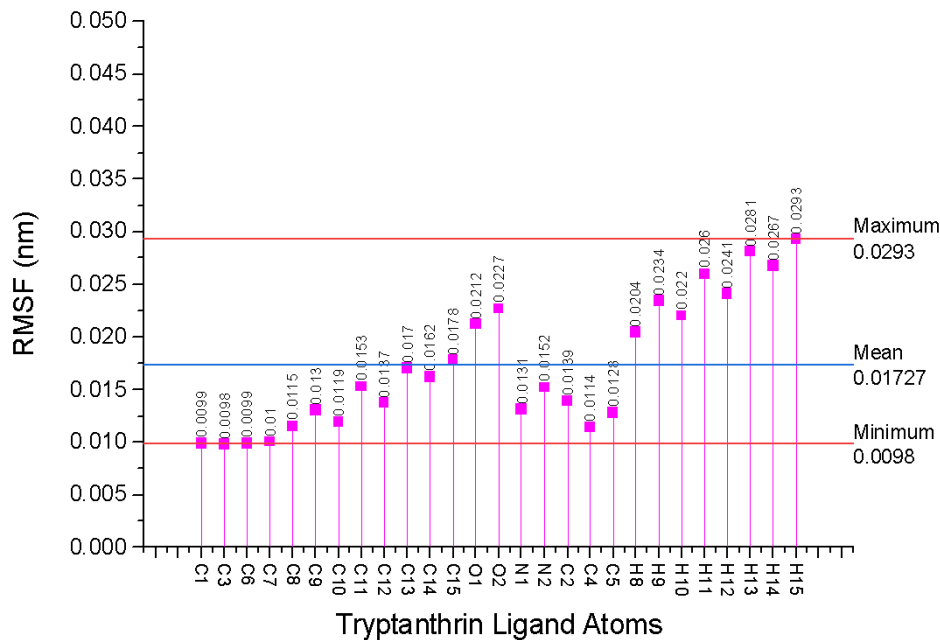


Figure 8: Total energy interactions profiles

In a protein's three-dimensional structure, RMSF is an average over the number of atoms measurement of how far an individual atom, or group of atoms, has moved away from the reference structure. The mean fluctuations of the ligand's atoms were 0.11904 nm for curcumin pyrazole, 0.05317 nm for scoparol, 0.01727 nm for tryptanthrin, 0.04734 nm for 4'-O-methylcatechin, and 0.11255 nm for omeprazole. As it is seen from these results tryptanthrin had minimum RMSF indicating that their atoms does not move far away from the reference structure. The maximum fluctuations of ligand's atoms are influenced by the environmental exposure. The minimum, mean and maximum fluctuations of the ligand's atoms are represented in Figure 9.





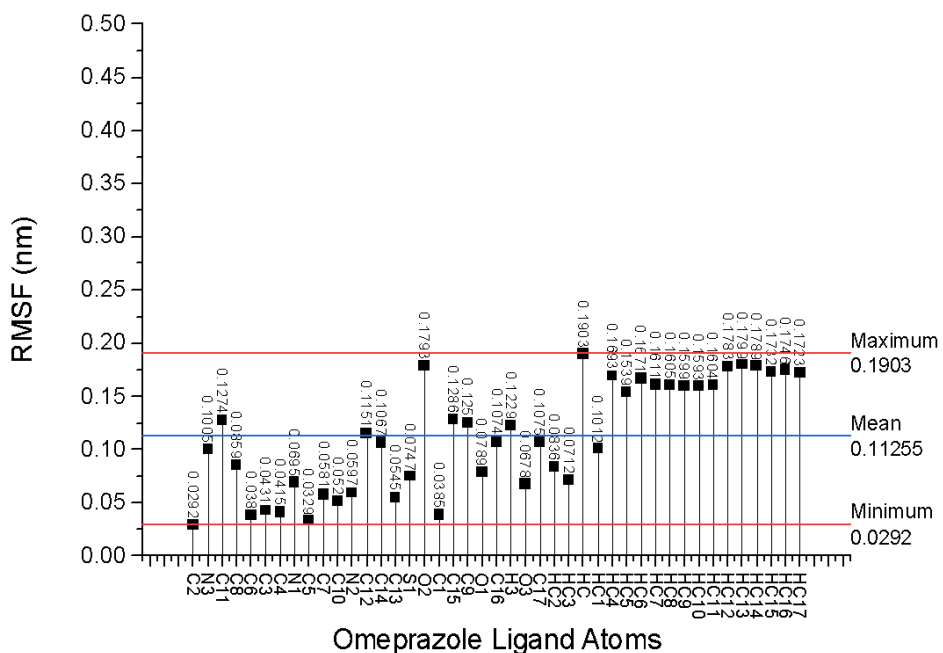


Figure 9: RMSF plots for curcumin pyrazole, scoparol, tryptanthrin 4'-O-methylcatechin, and Omeprazole.

The analysis of radius of gyration was used to determine the compactness of atoms in a structure under study. Thus, the radius of gyration tells about the distribution of atoms in the protein structure. The average values of radius of gyration for the five ligands are presented in Figure 10. As it is seen from Figure 10, tryptanthrin and 4'-O-methylcatechin had the minimum value of radius of gyration. This indicating that tryptanthrin (0.29 nm) and 4'-O-methylcatechin (0.375 nm) had minimum distribution of atoms along all axes, thus are stable inside the binding pocket (Chen et al., 2016). The analysis reveals that curcumin pyrazole binds in the active pocket of 8H52 with stable 2 – 3 H-bonds bonds formed in the time of 10 ns which also supports the docking findings. Scoparol initially had 4 - 5 unstable H-bonds formed with the target, at the end of 10 ns, 1 - 2 H - bonds remained stable, as a result, the decrement ends up with 2 strong H – bonds. For tryptanthrin, during molecular dynamics simulation, there were no stable hydrogen bonds formed in the run of 10 ns. This indicates that tryptanthrin is not stable in the binding pocket of 8H52. 4'-O-methylcatechin binds in the active pocket of 8H52 initially with 4 – 5 hydrogen bonds with fluctuations. It was also observed that a minimal stable of 2 - 3 H - bonds formed around 2 ns to 8 ns, from 8 ns till the end, 2 - 3 H - bonds remained stable for the 4'-O-methylcatechin - 8H52 complex. It was discovered that omeprazole binds in the active pocket of 8H52 with a total of 2 – 3 H - bonds with fluctuations initially. From 5 ns till the end, there were 1 – 2 stable H – bonds formed and makes a maximum of 2 H – bonds formed for the omeprazole – 8H52 complex (Figure 11), Therefore, 4'-O-methylcatechin formed 3 stable H-bonds indicating the stability in the binding pocket (Fatriansyah et al., 2022).

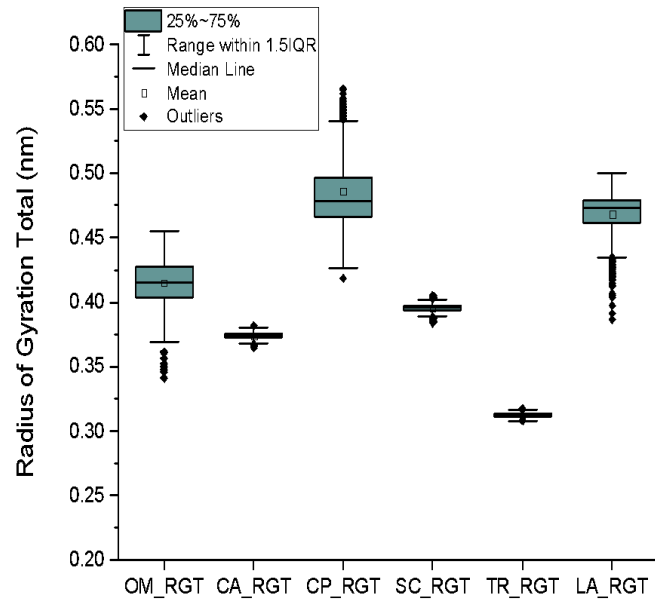
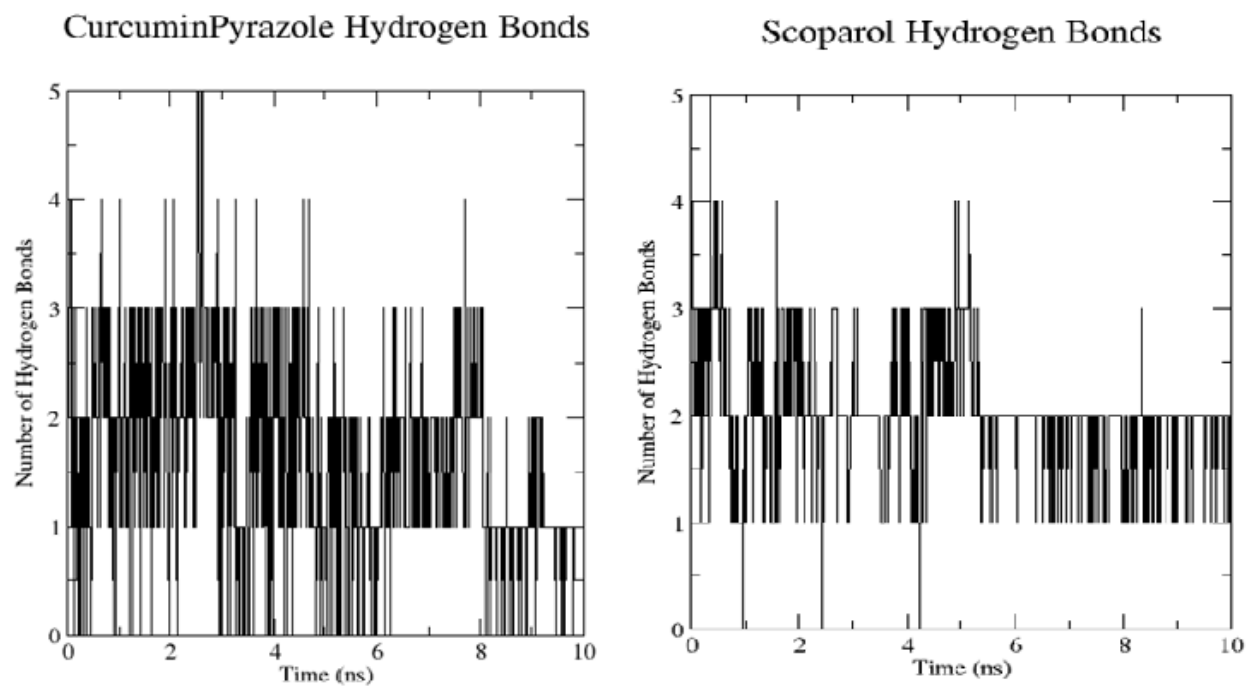


Figure 10: The average radius of gyration for the five hits



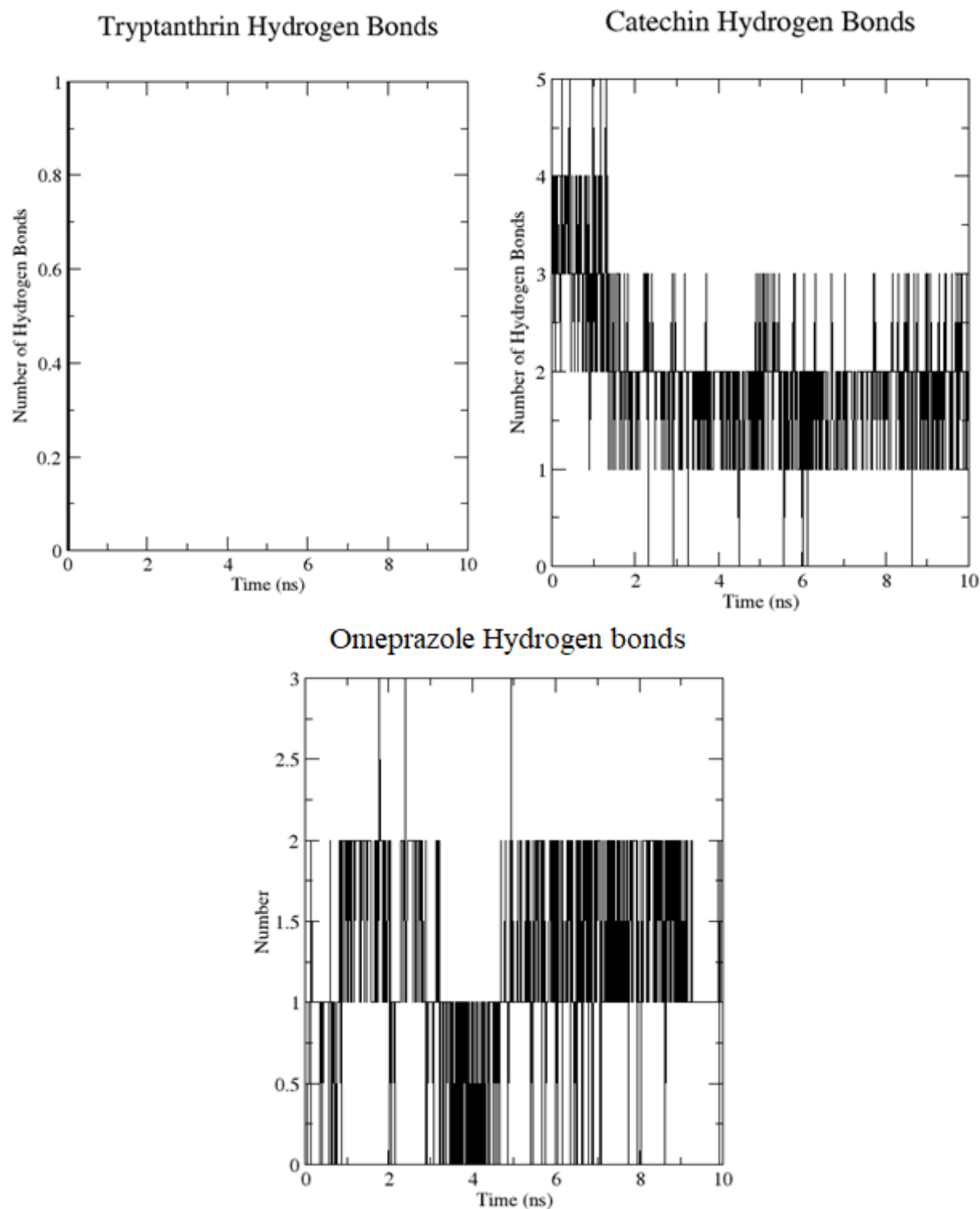


Figure 11: BACs and control drug hydrogen bonds

IV. CONCLUSION

In this study 1102 BACs from traditional medicinal herbs were investigated as a potential inhibitor for the treatment of peptic ulcers. Among those, four compounds curcumin pyrazole, scoparol, tryptanthrin, and 4'-O-methylcatechin were the ligands that outperformed Omeprazole were found to be promising for peptic ulcers treatment. Molecular docking results displayed docking scores of -9.9 Kcal/mol, -9.6 Kcal/mol, -9.5 Kcal/mol, -9.5 Kcal/mol, and -8.8 Kcal/mol for curcumin pyrazole, scoparol, 4'-O-methylcatechin, tryptanthrin, and omeprazole respectively. Therefore, these structures

have been identified to possess significant inhibitory activities against H-pylori. Further analysis was then performed using molecular dynamic studies to understand the flexibility and physical movement of the BACs and the control drug in complex with 8H52 as the target protein. Molecular dynamic results showed that all of the BACs had good findings. 4'-O-methycatechin had the best results compared to the control drugs in terms of binding affinity (-9.6 Kcal/mol), RMSD (0.18 nm), RMSF (0.04734 nm), H – bonds formed (2 to 3 stable H- bonds), and radius of gyration (0.375 nm). This study thus concludes that four BACs that were studied have inhibitory activities against 8H52, therefore these BACs are proposed to be possible candidates for medicines against 8H52 to inhibit bacterial growth and cell development to promote health and well-being for peptic ulcer disorders. MMPBSA, and other parameters such as temperatures, volume, bond energies, and lamb energies can be extended for further research to widen validation of results through in vitro and in vivo studies.

Funding: The authors express deep gratitude to University of Dodoma (UDOM) and Tanzania Atomic Energy Commission (TAEC) for supporting this work.

Conflict of interest: The authors disclose no conflict of interest.

REFERENCES

1. Ahmad, T., Cawood, M., Iqbal, Q., Ariño, A., Batool, A., Tariq, R. M. S., Azam, M., & Akhtar, S. (2019). Phytochemicals in *Daucus carota* and their health benefits. *Foods*, 8(9), 424.
2. Annapurna, A. (2012). Health benefits of amla or Indian gooseberry fruit (*Phyllanthus emblica*). *Asian Journal of Pharmaceutical Research and Health Care*, 4(4).
3. Anwer, K., Sonani, R., Madamwar, D., Singh, P., Khan, F., Bisetty, K., Ahmad, F., & Hassan, M. I. (2015). Role of N-terminal residues on folding and stability of C-phycoerythrin: simulation and urea-induced denaturation studies. *Journal of Biomolecular Structure and Dynamics*, 33(1), 121-133.
4. Baj, J., Forma, A., Sitarz, M., Portincasa, P., Garruti, G., Krasowska, D., & Maciejewski, R. (2020). *Helicobacter pylori* virulence factors—mechanisms of bacterial pathogenicity in the gastric microenvironment. *Cells*, 10(1), 27.
5. Bakchi, B., Krishna, A. D., Sreecharan, E., Ganesh, V. B. J., Niharika, M., Maharshi, S., Puttagunta, S. B., Sigalapalli, D. K., Bhandare, R. R., & Shaik, A. B. (2022). An Overview on Applications of SwissADME Web Tool in the Design and Development of Anticancer, Antitubercular and Antimicrobial agents: A Medicinal Chemist's Perspective. *Journal of Molecular Structure*, 132712.
6. Boltin, D., & Niv, Y. (2013). Mucins in gastric cancer—an update. *Journal of gastrointestinal & digestive system*, 3(123), 15519.
7. Castro-Alvarez, A., Costa, A. M., & Vilarrasa, J. (2017). The performance of several docking programs at reproducing protein–macrolide-like crystal structures. *Molecules*, 22(1), 136.
8. Charitos, I. A., D'Agostino, D., Topi, S., & Bottalico, L. (2021). 40 Years of *Helicobacter pylori*: a revolution in biomedical thought. *Gastroenterology Insights*, 12(2), 111-135.
9. Chen, D., Oezguen, N., Urvil, P., Ferguson, C., Dann, S. M., & Savidge, T. C. (2016). Regulation of protein-ligand binding affinity by hydrogen bond pairing. *Science advances*, 2(3), e1501240.
10. Coimbra, J. T., Feghali, R., Ribeiro, R. P., Ramos, M. J., & Fernandes, P. A. (2021). The importance of intramolecular hydrogen bonds on the translocation of the small drug piracetam through a lipid bilayer. *RSC advances*, 11(2), 899-908.
11. Elbehiry, A., Marzouk, E., Aldubaib, M., Abalkhail, A., Anagreyyah, S., Anajirih, N., Almuzaini, A. M., Rawway, M., Alfadhel, A., & Draz, A. (2023). *Helicobacter pylori* infection: current status and future prospects on diagnostic, therapeutic and control challenges. *Antibiotics*, 12(2), 191.

12. Fagoonee, S., & Pellicano, R. (2019). *Helicobacter pylori*: molecular basis for colonization and survival in gastric environment and resistance to antibiotics. A short review. *Infectious Diseases*, 51(6), 399-408.
13. Fatriansyah, J. F., Boanerges, A. G., Kurnianto, S. R., Pradana, A. F., & Surip, S. N. (2022). Molecular Dynamics Simulation of Ligands from Anredera cordifolia (Binahong) to the Main Protease (M pro) of SARS-CoV-2. *Journal of Tropical Medicine*, 2022.
14. FitzGerald, R., & Smith, S. M. (2021). An overview of *Helicobacter pylori* infection. *Helicobacter pylori*, 1-14.
15. Gapsys, V., Hahn, D. F., Tresadern, G., Mobley, D. L., Rampp, M., & de Groot, B. L. (2022). Pre-Exascale Computing of Protein–Ligand Binding Free Energies with Open Source Software for Drug Design. *Journal of chemical information and modeling*, 62(5), 1172-1177.
16. Gurusamy, K. S., & Pallari, E. (2016). Medical versus surgical treatment for refractory or recurrent peptic ulcer. *Cochrane Database of Systematic Reviews*(3).
17. Haley, K. P., & Gaddy, J. A. (2015). *Helicobacter pylori*: genomic insight into the host-pathogen interaction. *International journal of genomics*, 2015.
18. Hansson, T., Oostenbrink, C., & van Gunsteren, W. (2002). Molecular dynamics simulations. *Current opinion in structural biology*, 12(2), 190-196.
19. Hooi, J. K., Lai, W. Y., Ng, W. K., Suen, M. M., Underwood, F. E., Tanyingoh, D., Malfertheiner, P., Graham, D. Y., Wong, V. W., & Wu, J. C. (2017). Global prevalence of *Helicobacter pylori* infection: systematic review and meta-analysis. *Gastroenterology*, 153(2), 420-429.
20. Hussain, S. Z., Naseer, B., Qadri, T., Fatima, T., & Bhat, T. A. (2021). Plum (*Prunus domestica*): Morphology, Taxonomy, Composition and Health Benefits. In *Fruits Grown in Highland Regions of the Himalayas: Nutritional and Health Benefits* (pp. 169-179). Springer.
21. Iwu, M. W., Duncan, A. R., & Okunji, C. O. (1999). New antimicrobials of plant origin. *Perspectives on new crops and new uses*. ASHS Press, Alexandria, VA, 457, 462.
22. Kao, C.-Y., Sheu, B.-S., & Wu, J.-J. (2016). *Helicobacter pylori* infection: An overview of bacterial virulence factors and pathogenesis. *Biomedical journal*, 39(1), 14-23.
23. Ko, K. Y., Park, S. C., Cho, S. Y., & Yoon, S.-i. (2022). Structural analysis of carboxyspermidine dehydrogenase from *Helicobacter pylori*. *Biochemical and Biophysical Research Communications*, 635, 210-217.
24. Lim, S., Lee, E. J., & Kim, J. (2015). Decreased sulforaphene concentration and reduced myrosinase activity of radish (*Raphanus sativus* L.) root during cold storage. *Postharvest Biology and Technology*, 100, 219-225.
25. Lipinski, C. A. (2004). Lead-and drug-like compounds: the rule-of-five revolution. *Drug discovery today: Technologies*, 1(4), 337-341.
26. Motamarri, N. S., Karthikeyan, M., Rajasekar, S., & Gopal, V. (2012). *Indigofera tinctoria* Linn-a phytopharmacological review. *International Journal of Research in Pharmaceutical and Biomedical Sciences*, 3(1), 164-169.
27. Nath, A., & Joshi, S. (2013). Bioactivity assessment of endophytic fungi associated with the ethnomedicinal plant *Potentilla fulgens*. *World Journal of Pharmaceutical Research*, 2(6), 2596-2607.
28. Olaiya, C. O., & Soetan, K. O. (2014). A review of the health benefits of fenugreek (*Trigonella foenum-graecum* L.): Nutritional, Biochemical and pharmaceutical perspectives. *Int J Adv Social Sci Humanit*, 3-12.
29. Organization, W. H. (2004). *WHO guidelines on safety monitoring of herbal medicines in pharmacovigilance systems*. World Health Organization.
30. Peach, M. L., Cachau, R. E., & Nicklaus, M. C. (2017). Conformational energy range of ligands in protein crystal structures: the difficult quest for accurate understanding. *Journal of Molecular Recognition*, 30(8), e2618.

31. Peek, R. M., & Blaser, M. J. (2002). *Helicobacter pylori* and gastrointestinal tract adenocarcinomas. *Nature Reviews Cancer*, 2(1), 28-37.
32. Penta, R., De Falco, M., Iaquinto, G., & De Luca, A. (2005). *Helicobacter pylori* and gastric epithelial cells: from gastritis to cancer. *Journal of Experimental and Clinical Cancer Research*, 24(3), 337.
33. Pettersen, E. F., Goddard, T. D., Huang, C. C., Couch, G. S., Greenblatt, D. M., Meng, E. C., & Ferrin, T. E. (2004). UCSF Chimera—a visualization system for exploratory research and analysis. *Journal of computational chemistry*, 25(13), 1605-1612.
34. Preman, G., Mulani, M., Bare, A., Relan, K., Sayyed, L., Jha, V., & Pandey, K. (2022). Virtual Screening of Phytochemicals for Anti-Tubercular Potential Using Molecular Docking Approach.
35. Queiroz, D. M., Silva, C. I., Goncalves, M. H., Braga-Neto, M. B., Fialho, A. B., Fialho, A., Rocha, G. A., Rocha, A., Batista, S. A., & Guerrant, R. L. (2012). Higher frequency of cagA EPIYA-C phosphorylation sites in *H. pylori* strains from first-degree relatives of gastric cancer patients. *BMC gastroenterology*, 12(1), 1-7.
36. Qureshi, W. A., & Graham, D. Y. (2000). Antibiotic-resistant *H. pylori* infection and its treatment. *Current pharmaceutical design*, 6(15), 1537-1544.
37. Reddy Peasari, J., sri Motamarry, S., Varma, K. S., Anitha, P., & Potti, R. B. (2018). Chromatographic analysis of phytochemicals in *Costus igneus* and computational studies of flavonoids. *Informatics in Medicine Unlocked*, 13, 34-40.
38. Sabe, V. T., Ntombela, T., Jhamba, L. A., Maguire, G. E., Govender, T., Naicker, T., & Kruger, H. G. (2021). Current trends in computer aided drug design and a highlight of drugs discovered via computational techniques: A review. *European Journal of Medicinal Chemistry*, 224, 113705.
39. Sahoo, J. P., Behera, L., Praveena, J., Sawant, S., Mishra, A., Sharma, S. S., Ghosh, L., Mishra, A. P., Sahoo, A. R., & Pradhan, P. (2021). The golden spice turmeric (*Curcuma longa*) and its feasible benefits in prospering human health—a review. *American Journal of Plant Sciences*, 12(3), 455-475.
40. Salaria, D., Rolta, R., Mehta, J., Awofisayo, O., Fadare, O. A., Kaur, B., Kumar, B., Araujo da Costa, R., Chandel, S. R., & Kaushik, N. (2022). Phytoconstituents of traditional Himalayan Herbs as potential inhibitors of Human Papillomavirus (HPV-18) for cervical cancer treatment: An In silico Approach. *Plos one*, 17(3), e0265420.
41. Samanta, S. (2022). Potential bioactive components and health promotional benefits of tea (*Camellia sinensis*). *Journal of the American Nutrition Association*, 41(1), 65-93.
42. Schneider, G. (2013). Prediction of drug-like properties. In *Madame curie bioscience database [Internet]*. Landes Bioscience.
43. Singh, J., Jayaprakasha, G., & Patil, B. S. (2018). Extraction, identification, and potential health benefits of spinach flavonoids: A review. *Advances in Plant Phenolics: From Chemistry to Human Health*, 107-136.
44. Sjomina, O., Pavlova, J., Niv, Y., & Leja, M. (2018). Epidemiology of *Helicobacter pylori* infection. *Helicobacter*, 23, e12514.
45. Smoot, D. T. (1997). How does *Helicobacter pylori* cause mucosal damage? Direct mechanisms. *Gastroenterology*, 113(6), S31-S34.
46. Sowbhagya, H. (2014). Chemistry, technology, and nutraceutical functions of celery (*Apium graveolens L.*): an overview. *Critical reviews in food science and nutrition*, 54(3), 389-398.
47. Srinivasan, K. (2017). Ginger rhizomes (*Zingiber officinale*): A spice with multiple health beneficial potentials. *PharmaNutrition*, 5(1), 18-28.
48. Van den Brink, G., Tytgat, K., Van der Hulst, R., Van der Loos, C., Einerhand, A., Büller, H., & Dekker, J. (2000). *H pylori* colocalises with MUC5AC in the human stomach. *Gut*, 46(5), 601-607.
49. Vella, F. M., Cautela, D., & Laratta, B. (2019). Characterization of polyphenolic compounds in cantaloupe melon by-products. *Foods*, 8(6), 196.

50. Zhang, H., & Au, S. W. N. (2017). *Helicobacter pylori* does not use spermidine synthase to produce spermidine. *Biochemical and Biophysical Research Communications*, 490(3), 861-867.
51. Zhao, J., Cao, Y., & Zhang, L. (2020). Exploring the computational methods for protein-ligand binding site prediction. *Computational and structural biotechnology journal*, 18, 417-426.